

# **The First MEMS Platform for Creep and Stress Relaxation Tests on Polymeric, Metallic and Biological Nanofibers**

Mohammad Naraghi

Professor: Ioannis Chasiotis

University of Illinois at Urbana Champaign, IL

## **Abstract**

In this report, the operation principles and design steps of the components of a novel MEMS based mechanical testing platform for nanofibers are presented. While the device can be used to perform ordinary tension tests, its components are designed to specifically allow for creep/stress relaxation tests on nanofibers that demonstrate time dependent behavior, e.g. polymeric and biological nanofibers. In this platform, the samples are stretched by a comb drive actuator. The comb drive displacement is translated to the sample through an untethered shuttle. In order to engage the comb drive to the shuttle, two sets of teeth are symmetrically distributed on both sides of the shuttle, which are engaged with a pair of hooks connected to comb drive upon its actuation. To achieve constant deformation on the sample, specifically desired in stress relaxation tests, a pair of thermal actuators, referred to as thermal grips, are positioned on both sides of the shuttle, which grip the shuttle in its position when actuated. In addition, by proper sequencing of the electrical signals to the comb drives and thermal grips large deformations can be achieved, which can be used for mechanical characterization of highly deformable nanofibers. One of the key elements of this device is the on-chip, high stiffness and piezoresistivity based loadcell, which allows for load measurements in the order of micro- and sub microNewton forces in real time and at a fast rate. These features make the platform an ideal base for creep and relaxation tests. The device was designed to be fabricated by Sandia SUMMit process by using four polysilicon structural layers.

## **Objective**

This paper presents the physical principles and design steps for a MEMS tensile testing platform, to specifically perform creep and stress relaxation tests on polymeric nanofibers.

## **1. Introduction and Significance**

A common approach toward mechanical characterization of nanofibers and nanowires is tension test on individual samples [1-10]. For this purpose, MEMS devices have been widely used as testing platforms which provide grips to mount the samples and incorporate loadcells for microNewton level force measurement. In these platforms, the sample is loaded by on-chip [5-8,] or external actuators [11,12]. In general, on chip actuators are preferred over external actuators since they allow for highly accurate unidirectional sample loading.

The loadcells that are typically employed in such platforms are micromachined tethers with known stiffness, which are loaded in series with the test samples. The load in the sample is calculated by measuring the deformation of the tethers and multiplying by their stiffness [5,7,9-12], and it requires more compliant loadcells for better force resolution. In addition, in this approach, the displacement generated by the actuator is shared between the loadcell and the sample in the form of their deformations, in a ratio which is a function of the mechanical behavior of the sample, not known prior to performing the test, and the stiffness of the loadcell. As a result, the force and displacement in the sample are coupled, and following complete force controlled or displacement controlled protocols are not trivial.

In this paper, the design and operation principles of a novel MEMS tensile tester platform are presented which, unlike common MEMS devices discussed above, is capable of measuring micro- and nanoNewton range forces on the sample in real time and with no coupling between sample force and deformation by employing the piezoresistivity of polysilicon. In addition, the platform uses a comb drive actuator enhanced with thermal grips which allows for generating a fixed amount of deformation on the sample and also large deformations. The capacities of the platform makes it state of the art MEMS platform for performing stress relaxation and creep compliance tests on nanostructures, such as polymeric nanofibers, metallic nanowires and biological nanofibers, and therefore, significantly enhance the capabilities of MEMS tensile testing platforms.

## **2. Description of the MEMS Platform**

The MEMS device for creep and stress relaxation tests on nanoscale structures comprises of two main elements: the actuation element, and the force sensor. The whole design with its 3D drawn components is schematically shown in Figure 1. The right hand side of the design shows the method of actuation and the left hand side is the sample load sensor. To perform the test, a nanowires (sample) is mounted on the device with its two ends attached to the stationary and loading grips using a micro-manipulator with a sharpened probe [9]. By Application of appropriately sequenced electrical signals to the comb drive and the thermal grips, the shuttle is dragged and the sample is loaded.

As the sample stretches, the tensile force in the sample is transferred to the loadcell and deforms the loadcell, which is shown in Figure 2. This deformation changes the electrical resistance of the loadcell due to the piezoresistivity of the polysilicon, which can be used to measure the load.

### ***2.1. Comments on the Device Application***

While the device can be used to perform ordinary tensile tests on nanostructures similar to [9], the additional features such as the fixing mechanism on the actuator and the capability to measure force real time with high resolution, makes it ideal for creep and relaxation tests at nanoscale, for educational purposes and engineering measurements.

### 3. Principles of Operation

The main two components of the device are the actuator which is a combination of electrostatic and thermal MEMS actuators, and the piezoresistive based loadcell. The principles of operation of these components are explained here.

#### 3.1. Actuator: Lock, Drag, Grip Mechanism

The actuator is composed of an electrostatic actuator, a comb drive actuator, which drags an untethered shuttle in the sample loading direction, and a V-shaped thermal actuator, which is used to fix the position of the shuttle especially during a relaxation test. The steps of the operation of the actuator are shown in Figure 3. The actuation starts by applying a voltage difference on the comb drive between the fixed and moving sets of fingers, which generates an attractive electrostatic force between the two sets of fingers. This attraction force pulls the moving set of fingers and with that the clamping beams and the hooks to the right. Therefore, the hooks get engaged with the interlocking teeth, and the shuttle is dragged to the right.

In order to keep the deformation constant, for instance in a stress relaxation test, a pair of V-shaped thermal actuators are placed on both sides of the shuttle, figure 1. By passing an electrical current through the thermal actuators, they get expanded due to Joule heating, and since the legs are inclined, Figure 4, the thermal grips move vertically toward the shuttle [13], until physical contact. The grip mechanism keeps the deformation constant, and the comb drive actuator can be set free. In this stage, due to the spring force in the comb drive tethers, the hook of the clamping beams will hit the inclined (or back) side of the shuttle teeth. The back side of the teeth should be inclined so much that it does not prohibit the backward motion of the comb drive to its rest position. For further deformations, the thermal grips should be released, and simultaneously the comb drive should be actuated again to further drag the shuttle. This cycle can be continued until desired amount of deformation is reached.

#### 3.2. Piezoresistive PolySilicon Loadcell

The relative change in resistance of an alloy or semiconductor bar when it is subjected to strain  $\varepsilon$  can be estimated as:

$$\frac{\Delta R}{R} = S \varepsilon \quad (1)$$

where  $S$  is the sensitivity of the bar defined as:

$$S = 1 + 2\nu + \frac{d\rho/\rho}{\varepsilon} \quad (2)$$

In this equation,  $\nu$  is the poison ratio, and  $\rho$  is the specific resistivity. For typical alloys, the last term in equation 2 is negligible, while for semiconductors this term is substantial, between -125 to 175 depending on the type and concentration of the impurity [14]. The loadcell used in this

design works based on the changes in the resistance caused by the force applied on the loadcell through the sample, and its consequent strain.

## 4. Modeling of Proposed Device

Different aspects of modeling and analysis of the design are discussed in this section briefly.

### 4.1. Actuator

The actuator comprises of a comb drive actuator and a pair of thermal grips which get engaged with an untethered shuttle.

#### 4.1.1 Pulling Mechanism: Comb Drive Actuator

The driving force on the shuttle comes from the comb drive actuator, in which electrostatic force is generated between the moving and stationary fingers by applying a biased voltage between them,  $V$ , that moves the moving fingers toward the stationary fingers. Part of the electrostatic force is absorbed by the tethers while the rest is transferred to the shuttle,  $F_{net}$  in equation 3:

$$F_{net} = \frac{Nh\epsilon_0 V^2}{g} - n_t P_{(\delta)} \quad (3)$$

in which,  $P_{(\delta)}$  is the lateral force in the tethers as a function of travel length,  $\delta$ , in the x direction, Figure 1,  $n_t$  is the number of the tethers,  $h$  is the height of the fingers and  $g$  is the distance between the moving and stationary fingers. The voltage in this equation is limited by the pull in instability voltage which can be estimated from equation 4 [15].

$$\frac{k_y}{1 + \frac{3}{8} \left( \frac{\Delta}{w} \right)^2} = \frac{4\epsilon_0 N V_{pull-in}^2 h(l_i + \delta)}{g^3} \quad (4)$$

in which  $l_i$ ,  $k_y$  and  $w$  are the initial overlap between the fingers, axial stiffness of the tethers and width of the tethers respectively. The design of the comb drive should be such that it allows for the application of the desired net force on the sample, 25  $\mu$ N, throughout the tension experiment while the voltage is kept below the pull in instability. Specifications for the tethers and fingers which satisfy the above condition are calculated and presented in Table 1.

#### 4.1.2 Gripping Mechanism

As discussed in section 3, two thermal actuators are considered for gripping the shuttle. The thermal actuators consist of V shaped beams arranged parallel to each other, and anchored on both sides, Figure 1 and 4. A detailed description of these actuators and their operation principle can be found in [7].

## 4.2. Modeling of Loadcell Operation

The loadcell consists of several tensile and compressive bars which act in series in response to the applied load by change in their resistance. The loadcell is anchored to the substrate from one side at point B, Figure 2. For electrical connections and mechanical stability the other side of the loadcell is connected to a pair of tethers, Figure 2. The tethers and the loadcell are in parallel to each other. A simple electromechanical analysis of the loadcell reveals that an applied force of  $F$  results in a change in resistance of  $\Delta R$ , which are related as:

$$\Delta R = \frac{S\rho LF}{2Eh^2} \left[ \left( \frac{n}{2} + 1 \right) \frac{1}{w_t^2} - \frac{n}{2} \frac{1}{w_w^2} \right] \quad (5)$$

where  $E$  is the polysilicon elastic modulus, 162.5 GPa. In addition,  $\varepsilon$  and  $S$  are the axial strain in the bars and the gage factor of polysilicon. The latter is between -175 to 125, based on the concentration of the contaminant in the polysilicon. In the SUMMIT© process, polysilicon is P-doped, therefore, here it is assumed  $S \approx 100$ , and  $\rho$  is the specific resistivity of polysilicon. It is needless to mention that an accurate measure of  $S$  can be found by calibrating the loadcell. As shown in Figure 5. From equation 15, the following trends are extracted:

- The change in resistance scales inversely with the square of width. Therefore, the ratio of 4 for the width of wide tethers to thin tethers (4  $\mu\text{m}$  to 1  $\mu\text{m}$ ) significantly reduces the adverse effect of wide bars in reducing the change in resistance.
- In order to improve the sensitivity of the device in measuring the force as a function of change in resistance, the following is beneficial:
  - Increasing the length of the bars,  $L$
  - Increasing the number of pairs of bars,  $n$
  - Decreasing the width of the thin bars,  $w_t$

Therefore, the following values were chosen in this design:  $L = 200\mu\text{m}$ ,  $n = 2$ ,  $w_t = 1\mu\text{m}$

Further increase of  $L$  and  $n$ , and decrease in  $w_t$  lowers the fabrication reliability. Like  $w_t$ , further increase in  $L$  and  $n$ , and decrease in  $w_t$  is not pursued here due to the risk of fabrication failure.

## 5. Summary

A novel and first of its kind MEMS tension testing platform designed specifically to perform creep and stress relaxation tests on polymeric nanofibers was presented here. For the first time, the device highly benefits from the piezoresistivity of polysilicon for real time measurement of micronewtons range sample forces. In addition, the MEMS loadcell can be used as a part of a Wheatstone bridge, which significantly increases the load measurement resolution. The high stiffness of the loadcell does not allow for coupling of the sample force and deformation, which one faces in case of typical MEMS leafspring loadcells. For actuation, a set of electrostatic and capacitive actuators, known as comb drives and V-shaped thermal actuators, are incorporated. The coordinated actuation of the actuators drags an untethered shuttle which in turn stretches the

nanoscale sample. The analysis provided in this text, confirms the capability of current device for time dependent mechanical characterization experiments.

## Appendix 2: Figures and Tables

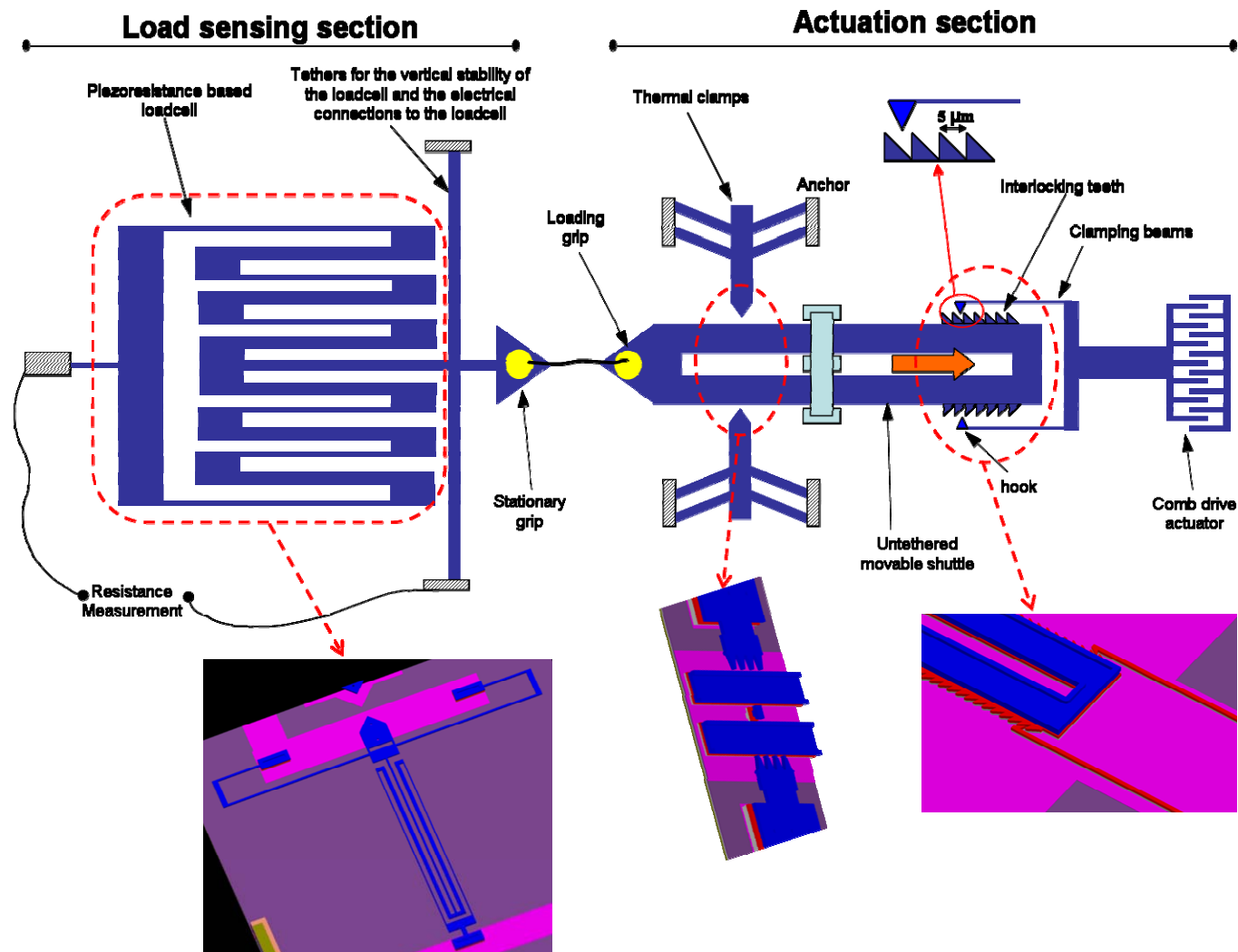


**Figure 1.** The schematic of the creep/relaxation testing platform with the 3D view of its components

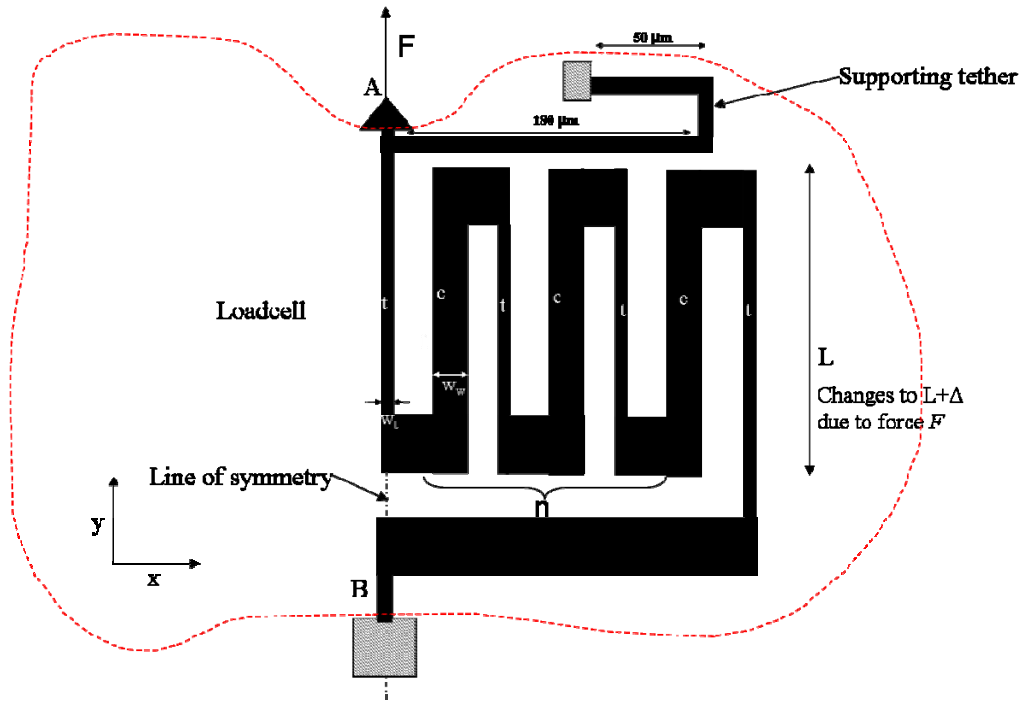


**Figure 2.** Schematic of the piezoresistive based loadcell

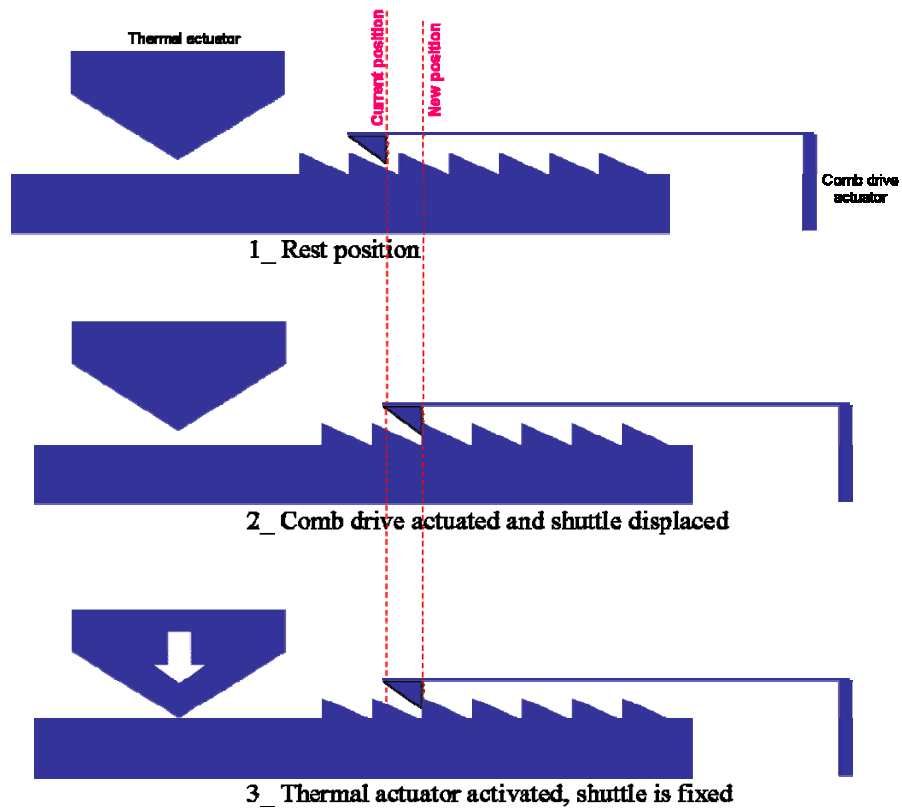


**Figure 3.** Operation steps of the actuator



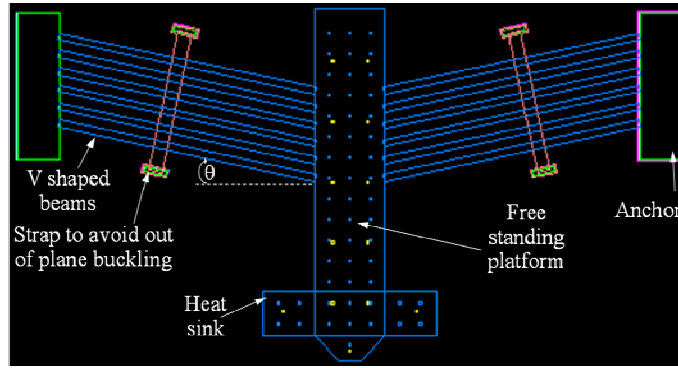


**Figure 4.** The V shaped thermal actuators used as thermal grips

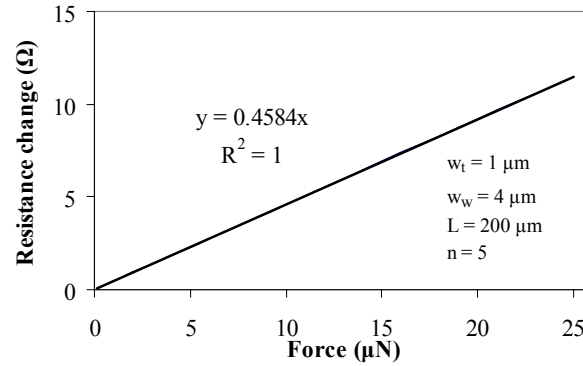


**Figure 5.** Variation of the resistance as a function of force for the piezoresistive loadcell

**Table 1.** Geometrical specifications of the comb drive actuators

Number of tethers, $n_t$	6
Number of pair of fingers, $N$	100
Tether length, $\mu\text{m}$	460
Tether width, $\mu\text{m}$	2

## 6. Reference

- [1] Ko F, Gogotsi Y, Ashraf A, Naguib N, Ye H, Yang G, Li C and Willis P 2003 *J. Adv. Mater.* **15** 1161-5
- [2] Cuenot S, Demoustier-Champagne S and Nysten B 2000 *Phys. Rev. Lett.* **85** 1690-3
- [3] Zussman E, Chen X, Ding W, Calabri L, Dikin D A, Quintana J P and Ruoff R S 2005 *J. Carbon* **43** 2175–85
- [4] Yu M F, Atashbar M S and Chen X 2005 *J. IEEE Sensors* **5** 20-5
- [5] Haque M A and Saif M T A 2003 *J. Soc. Exp. Mech.* **43** 248-55
- [6] Lu S, Guo Z, Ding W and Ruoff R S 2006 *J. Rev. Sci. Instrum.* **77** 056103 (1-4)
- [7] Zhu Y, Moldovan N and Espinosa H D 2005 *Appl. Phys. Lett.* **86** 013506(1-3)
- [8] Kiuchi M, Isono Y, Sugiyama S, Morita T and Matsui S 2005 *Proceedings of 2005 5th IEEE Conference on Nanotechnology, Nagoya, Japan*
- [9] M. Naraghi, I. Chasiotis, Y. Dzenis, Y. Wen, and H. Kahn, *Rev. Sci. Instrum.* **78** 085108-1 (2007).
- [10] M. Naraghi, I. Chasiotis, Y. Dzenis, Y. Wen, and H. Kahn, *Appl. Phys. Lett.* (2007).
- [11] Samuel B A, Haque M A, Yi B, Rajagopalan R and Foley H C 2007 *J. nanotechnology* **18** 1-8
- [12] Naraghi M, Chasiotis I, Wen Y and Dzenis Y *Proceedings of 2007 SEM conference, Springfield, MA*
- [13] Zhu Y Moldovan N and Espinosa H D 2005 *Appl. Phys. Lett.* **86** 013506(1-3)
- [14] J. W. Dally and W. F. Riley “Experimental stress analysis”, 3rd edition, Knoxville, Tennessee.
- [15] Chen C and Lee C 2004 *J. Sensors and Actuators* 530-539